

NONLINEAR MECHANISMS OF THE INITIAL STAGE OF THE LAMINAR–TURBULENT TRANSITION AT HYPERSONIC VELOCITIES

A. N. Shpilyuk,¹ D. A. Bountin,¹ A. A. Maslov,¹ and N. Chokani²

UDC 532.526

Weakly nonlinear development of waves in an axisymmetric hypersonic boundary layer is studied by the method of bispectral analysis. The type of nonlinear interaction that was not observed previously in such flows is found. The possibility of subharmonic resonance of the second mode at the nonlinear stage of transition is demonstrated. The previously discovered nonlinear generation of the harmonic of the fundamental wave of the second mode of disturbances is observed.

Key words: *hypersonic, boundary layer, nonlinear interaction, bispectral analysis, bicoherence.*

Introduction. The knowledge of the laminar–turbulent transition point is very important for aircraft and rocket construction because skin friction and heat transfer between the vehicle and the ambient medium significantly depend on the boundary-layer flow regime. The nonlinear stage of transition is the final one and follows the stage of receptivity (where the external flow oscillations are transformed into the own oscillations of the boundary layer) and the stage of linear development of disturbances (described by the linear stability theory). Nonlinear interaction leads to the formation of phase-related waves, which results in laminar-flow stochastization manifested in energy redistribution in the power spectrum of flow oscillations. It is found that one of the main types of nonlinear interaction at the initial stage of nonlinearity at subsonic velocities is the subharmonic (parametric) resonance [1, 2]. In this type of interaction, the wave with the frequency equal to one half of the frequency of the fundamental wave (subharmonic) is nonlinearly amplified.

It is shown in [3] that the subharmonic resonance is the main mechanism in the weakly nonlinear region of transition in a supersonic boundary layer. The evolution of the first mode waves, which have a vortex nature and are dominating up to Mach numbers $M \approx 4$, was considered [4]. The method of artificial wave packets was used in the experiments of [5, 6], which allowed a detailed study of wave processes in the boundary layer.

In analyzing natural disturbances, effects of nonlinearity can be revealed by several methods. One of the most widely used techniques is the statistical method. It is based on the fact that the distribution of signal fluctuations close to the Gaussian distribution (in the general case, the distribution symmetry) means that the process is linear (the harmonics composing the signal are linearly independent), whereas any significant deviation from the normal distribution characterizes the process nonlinearity [7, 8]. The drawback of the statistical method is that it does not allow obtaining any particular characteristics of the nonlinear process. Not only to reveal the effect of nonlinearity but also to determine which waves are nonlinearly related and also to find the degree of this relation, the bispectral analysis is used (though for quadratic nonlinearity only). In [9], both methods were used to study the nonlinear stage of the laminar–turbulent transition in a supersonic boundary layer on a flat plate. The results of statistical and bispectral analysis were in good agreement.

In [8, 10], the bispectral analysis was used to study nonlinear interaction of waves in the weakly nonlinear region of transition in hypersonic boundary layers, where two-dimensional (the wave vector is parallel to the flow direction) second-mode disturbances with an acoustic nature are dominating [4]. In studying the transition at

¹Institute of Theoretical and Applied Mechanics, Siberian Division, Russian Academy of Sciences, Novosibirsk 630090. ²State University of North Carolina, Raleigh 27695, USA. Translated from *Prikladnaya Mekhanika i Tekhnicheskaya Fizika*, Vol. 44, No. 5, pp. 63–70, September–October, 2003. Original article submitted March 31, 2003.

hypersonic velocities, a new type of nonlinear interaction differing from subsonic and supersonic cases was observed, namely, generation of the harmonic of the fundamental wave (wave with a frequency twice as high as the frequency of the fundamental wave) [8, 10, 11]. No proof of the presence of subharmonic resonance was found.

It is known that the laminar–turbulent transition in wind tunnels can occur in a different manner because of the different level and spectral composition of free-stream noise. Therefore, it is necessary to perform experiments in different wind tunnels to make sure that the observed phenomenon is a specific feature of a given type of flow rather than of a particular facility. The data of [8, 10] were obtained for different mean and fluctuating free-stream parameters, and the analysis of the measurement results indicates the presence of one mechanism of nonlinearity: generation of the harmonic of the fundamental wave. The available data, however, are insufficient to draw the final conclusions on the mechanisms of nonlinear evolution of disturbances at hypersonic velocities.

The objective of the present work is to obtain additional experimental data on evolution of disturbances in the weakly nonlinear region of transition in hypersonic boundary layers by the method of bispectral analysis.

1. Experimental Equipment. The experiments were performed in a T-326 hypersonic blowdown wind tunnel based at the Institute of Theoretical and Applied Mechanics of the Siberian Division of the Russian Academy of Sciences for a free-stream Mach number $M_\infty = 5.95$, unit Reynolds number $Re_{1\infty} = 11.9 \cdot 10^6 \text{ m}^{-1}$, stagnation pressure $P_0 = 10^6 \text{ Pa}$, and stagnation temperature $T_0 = 390 \text{ K}$. During the test, the values of the parameters P_0 and T_0 were maintained constant within 0.06 and 0.25%, respectively. The free-stream parameters M_∞ and $Re_{1\infty}$ were determined by the measured values of P_0 and T_0 and the known dependence $M_\infty = f(P_0)$ obtained in studying the flow field in the test section of the T-326 wind tunnel. Mass-flow fluctuations ρu (ρ is the density and u is the flow velocity) were measured by a constant-current hot-wire anemometer operating in the range of frequencies 0–600 kHz. Single-wire probes 1 mm long were used; the probes were made of tungsten wire 5 μm in diameter.

The mass-flow fluctuations were measured in the layer where their values were maximum [12]. The error of hot-wire motion across the boundary layer was 0.01 mm. The x coordinate was counted along the cone generatrix from the model tip, and the error of motion in the x direction was 0.02 mm.

During the experiment, the variable component of the electric signal from the hot-wire output was recorded into the PC memory through a 12-bit ADC. To obtain the spectra of fluctuations, the variable signal was digitized with a frequency of 5 MHz, which allowed us to analyze signals up to a frequency of 2.5 MHz. Because of the limited spectral range of the hot-wire anemometer, however, data lower than 600 kHz were used.

The model was a sharp steel cone 0.5 m long with a half-angle of 7° . The bluntness radius of the model tip was smaller than 0.1 mm. The model was mounted at zero incidence (within 0.06°).

2. Bispectral Analysis. The bispectrum definition can be explained using an analogy with the signal-power spectrum. The power spectrum is the Fourier transform of the autocorrelation function

$$P(f) = \int_{-\infty}^{\infty} R_{2x}(\tau) \exp(-i2\pi f\tau) dt = X^*(f)X(f),$$

where $R_{2x}(\tau) = \lim_{T \rightarrow \infty} \frac{1}{T} \int_{-T/2}^{T/2} x(t)x(t+\tau) dt$ is the autocorrelation function or a cumulant (moment) of the second order and $X(f)$ is the Fourier transform of the signal $x(t)$; the superscript asterisk indicates complex conjugation.

The bispectrum is a double Fourier transform of the second-order autocorrelation function [13]

$$B(f_1, f_2) = \int_{-\infty}^{\infty} \int_{-\infty}^{\infty} R_{3x}(\tau, \lambda) \exp(-i2\pi f_1\tau) \exp(-i2\pi f_2\lambda) d\tau d\lambda = X^*(f_1 + f_2)X(f_1)X(f_2),$$

where $R_{3x}(\tau, \lambda) = \lim_{T \rightarrow \infty} \frac{1}{T} \int_{-T/2}^{T/2} x(t)x(t+\tau)x(t+\lambda) dt$ is the third-order cumulant.

Since the bispectrum amplitude depends on the wave amplitude, the bispectrum is usually normalized to the power spectrum, which yields the bicoherence spectrum

$$\text{bic}^2(f_1, f_2) = \frac{|B(f_1, f_2)|^2}{P(f_1)P(f_2)P(f_1 + f_2)}.$$

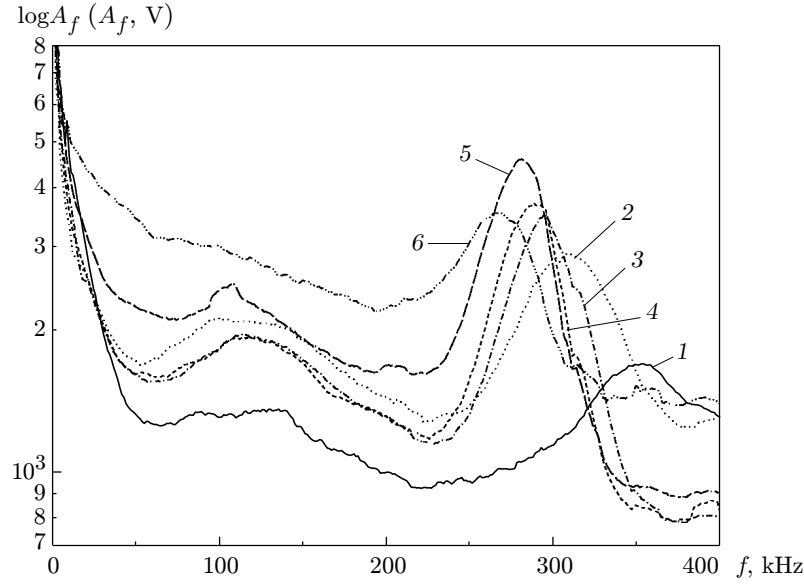


Fig. 1. Fourier spectrum of the signal A_f in the layer of the maximum fluctuations for $x = 200$ (1), 245 (2), 269 (3), 286 (4), 304 (5), and 315 mm (6).

The bicoherence amplitude can be interpreted as the contribution of energy of nonlinear interaction to the wave energy with a frequency $f_1 + f_2$ or as the power of the quadratic relation in terms of wave phases $f_1, f_2, f_3 = f_1 + f_2$. The bicoherence amplitude is limited by the values of 0 (completely independent waves) and 1 (completely related waves).

In practice, averaging is used to obtain a good signal-to-noise ratio for bicoherence amplitudes. The digitized signal is divided into M sectors, the bispectrum and power spectrum are calculated for each sector, averaging in terms of M is performed, and the bicoherence is finally obtained:

$$\text{bic}^2(f_1, f_2) = \frac{1}{M} \sum_{i=1}^M |B_i(f_1, f_2)|^2 \left[\frac{1}{M^3} \sum_{i=1}^M P_i(f_1) \sum_{i=1}^M P_i(f_2) \sum_{i=1}^M P_i(f_1 + f_2) \right]^{-1}.$$

The condition of phase relation of three waves f_1, f_2, f_3 is

$$f_3 = f_1 + f_2, \quad \varphi_3 = \varphi_1 + \varphi_2.$$

If the waves are statistically independent, all phases are random quantities, and the bicoherence amplitude after averaging tends to zero. If the waves satisfy the above-described conditions, the bicoherence amplitude tends to unity.

Owing to bispectrum (and bicoherence) symmetry, it is sufficient to know its value in the triangle $(0, 0), (f_N, 0), (f_N/2, f_N/2)$, where f_N is the Nyquist frequency (see [13] for more details). In the present work, the graphs are plotted in the region $0 < f_1 < 600$ kHz, $0 < f_2 < 600$ kHz (the upper limit is associated with the frequency range of the hot-wire anemometer), providing redundant information (the plots are symmetric about the line $f_1 = f_2$). In the authors' opinion, this representation makes the data more understandable. If the plot has a peak at the intersection of frequencies (f_1, f_2) , this means that waves with the frequencies $f_1, f_2, f_3 = f_1 + f_2$ are nonlinearly related. Nevertheless, the bicoherence spectrum does not contain information about the particular type of interaction: $f_3 - f_1 \rightarrow f_2, f_3 - f_2 \rightarrow f_1$, or $f_1 + f_2 \rightarrow f_3$. Correct interpretation of data requires a physical analysis or additional information (e.g., the Fourier spectrum of the signal).

In the present work, the bicoherence spectra were calculated on the basis of records with 2^{17} samples. For averaging, the record was divided into 512 time series with 256 samples in each. The frequency resolution for the bicoherence spectra was 20 kHz.

3. Results and Discussion. Figure 1 shows the Fourier spectra of the signal for six cross sections along the x coordinate. Two regions with the centers at $f \approx 110$ kHz and $f \approx 350$ – 270 kHz are clearly seen, which correspond to disturbances of the first (vortex) and second (acoustic) modes. The amplitude of the second-mode waves is higher than that of the first-mode waves, since the second-mode disturbances are more unstable for this type of flows.

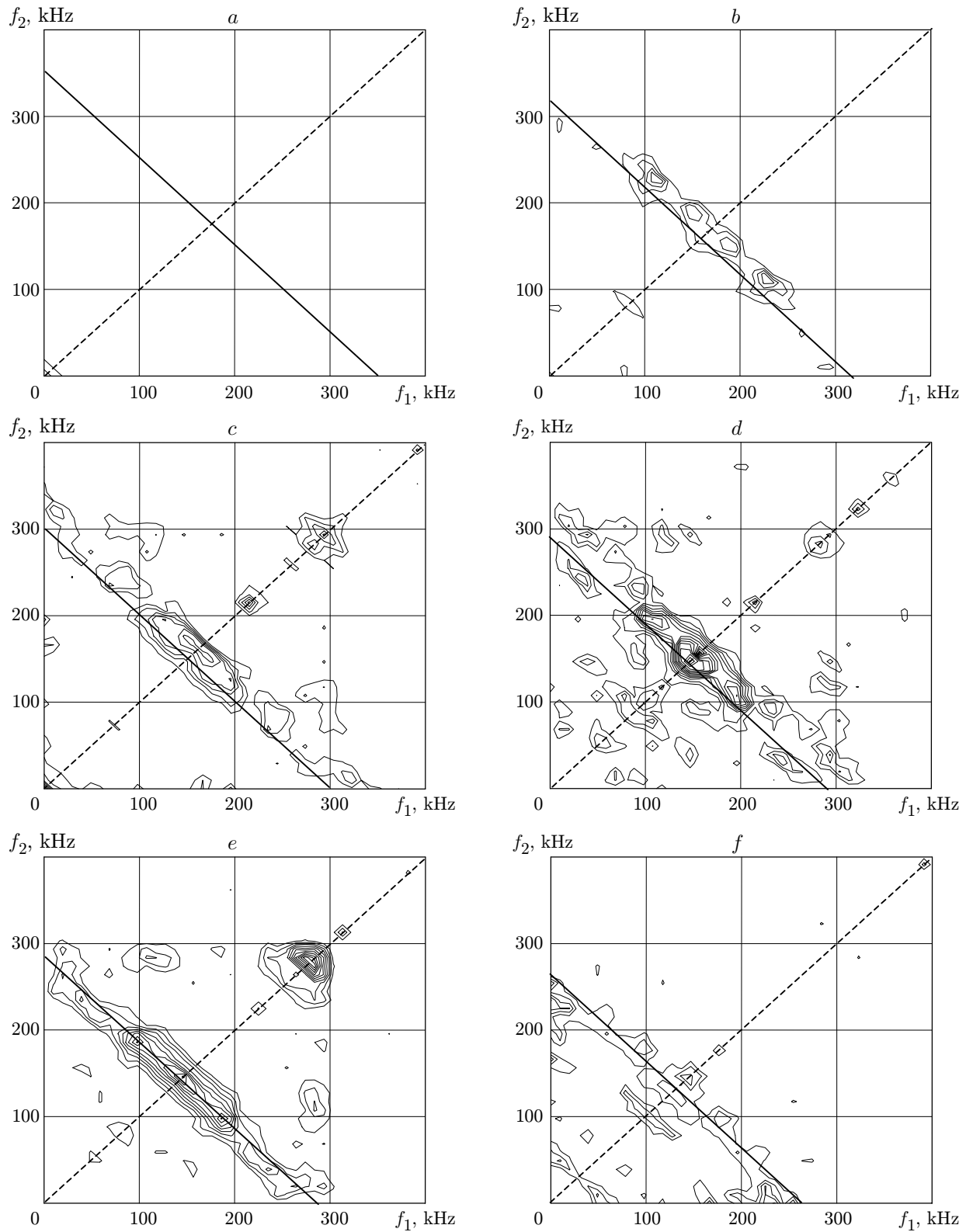


Fig. 2. Spectrum of signal bicoherence in the layer of the maximum fluctuations for $x = 200$ (a) 245 (b), 269 (c), 286 (d), 304 (e), and 315 mm (f): the solid curves refer to $f_1 + f_2 = f_{II}$ and the dashed curves refer to $f_1 = f_2$.

For the same cross section, Fig. 2 shows the bicoherence spectra (the dashed line is the line of symmetry of the plot; the solid line is defined by the equation $f_1 + f_2 = f_{II}$, where f_{II} is the frequency of the local maximum in the Fourier spectrum of the signal corresponding to the second mode of disturbances; the isolines are plotted from the level of 0.03 with a step of 0.021).

In the first cross section $x = 200$ mm ($Re = Re_{1e} x = 3.17 \cdot 10^6$, where Re_{1e} is the unit Reynolds number based on parameters at the boundary-layer edge), there are no peaks in the bicoherence spectrum ($bic^2 < 0.03$), i.e., the disturbances develop linearly (Fig. 2a).

Beginning from the cross section $x = 245$ mm ($Re = 3.87 \cdot 10^6$), nonlinearly related waves appear (Fig. 2b). The interaction occurs in a wide range of frequencies along the line $f_1 + f_2 \approx 335$ kHz. The total frequency of interaction is somewhat higher than the center of the second-mode frequency packet $f_{II} \approx 320$ kHz (see Fig. 1) but within the frequency resolution. Thus, three waves are phase-related: f_1 , f_2 , and $f_3 = f_1 + f_2 \approx f_{II}$. The peak $(f_1, f_2) = (110 \text{ kHz}, 230 \text{ kHz}) \approx (f_I, f_{II} - f_I)$ (f_I corresponds to the center of the first-mode frequency packet) is noticeable in all cross sections in the downstream direction, except for the cross section $x = 269$ mm ($Re = 4.24 \cdot 10^6$) (Fig. 2c). Apparently, the formation of this peak is related to the fact that there is a local maximum in the Fourier spectrum in the vicinity of $f \approx 110$ kHz (see Fig. 1). In the cross section $x = 269$ mm, the bicoherence amplitude increases, the interaction also occurs along the line, but the line is slightly displaced toward lower frequencies $f_1 + f_2 \approx f_{II} \approx 320$ kHz. Such a displacement is also observed in other cross sections (Fig. 2d–f), which is associated with the downstream decrease in the second-mode frequency (this is seen in the Fourier spectra). The center of interaction [a local maximum at the frequency $(f_{II}/2, f_{II}/2)$] is clearly traced up to the strongly nonlinear region (Fig. 2f). Identification of the second-mode subharmonic (which is better noticeable in the subsequent cross sections) synchronized with the fundamental wave is one of the signs of the subharmonic resonance. Yet, this can be a simple combination interaction if not all conditions of the resonance are satisfied. Note, for the resonance to exist, one should satisfy the equalities

$$f_{1/2,1} + f_{1/2,2} = f_0, \quad \varphi_0 = \varphi_{1/2,1} + \varphi_{1/2,2}$$

(f_0 is the frequency of the fundamental wave and $f_{1/2}$ is the frequency of the subharmonic wave) and the conditions on the wavenumbers

$$\alpha_{1/2,1} + \alpha_{1/2,2} = \alpha_0, \quad \beta_{1/2,1} + \beta_{1/2,2} = \beta_0$$

[α and β are the longitudinal and transverse (in our case, circumferential) wavenumbers]. It does not seem possible to verify satisfaction of the last two equalities in the present work. Therefore, it is possible to determine whether a given interaction is resonance or simply combination only by performing additional studies. It is known, however, that the streamwise phase velocity of the second-mode waves depends weakly on the wave inclination angle [14]; therefore, the condition $\alpha_{1/2} + \alpha_{1/2} = \alpha_0$ should be satisfied for waves in a wide range of angles. In our case, $\beta_0 = \beta_{II} = 0$ (because of the two-dimensionality of the most unstable second-mode disturbances), and we have $\beta_{1/2,1} = -\beta_{1/2,2}$, which corresponds to a pair of symmetric waves. Thus, the interacting wave triplet is close to the triplet observed at subsonic velocities [1].

The presence of a wide frequency range of interacting waves does not contradict the existence of the resonance. In the case of subsonic velocities, the subharmonic resonance exists with a frequency detuning $f_{1/2} \pm \Delta f$ until $\Delta f = f_{1/2}$ [1], and phase synchronism of waves participating in the resonance was observed in a wide range of frequencies up to the fundamental wave frequency f_0 [15].

In the cross section $x = 269$ mm (Fig. 2c), a new type of interaction appears at the frequency $(f_1, f_2) = (300 \text{ kHz}, 300 \text{ kHz}) \approx (f_{II}, f_{II})$, i.e., the harmonics of the second-mode waves are generated due to nonlinear mechanisms: $(f_1 \approx f_{II}) + (f_2 \approx f_{II}) \rightarrow (f_3 \approx 2f_{II})$. This type of interaction was observed previously and was described in [8, 10]. In subsequent cross sections, the level of bicoherence continues to grow and reaches the maximum value $bic^2 \approx 0.35$ at $x = 287$ mm ($Re = 4.53 \cdot 10^6$) (Fig. 2d). The line of interaction moves toward lower frequencies even further: $f_1 + f_2 \approx 290$ kHz. New regions of phase-related waves appear around the line of interaction and also in the low-frequency region. In particular, the following peaks can be identified: $(f_1, f_2) = (110 \text{ kHz}, 110 \text{ kHz}) \approx (f_I, f_I)$ — interaction of the first-mode waves with waves whose frequency is approximately equal to $2f_I$; $(f_1, f_2) = (45 \text{ kHz}, 145 \text{ kHz}) \approx (f_I/2, f_{II}/2)$ — phase synchronization of subharmonics of the first and second modes with the wave of the total frequency of 200 kHz; $(f_1, f_2) = (55 \text{ kHz}, 55 \text{ kHz}) \approx (f_I/2, f_I/2)$ — interaction of the first-mode subharmonic with the first-mode fundamental wave. The interaction mechanism considered is, apparently, similar to that found at supersonic velocities [3].

In the next cross section ($x = 304$ mm), the interaction amplitude $f_{II} + f_{II} \rightarrow 2f_{II}$ is maximum ($\text{bic}^2 \approx 0.26$), but the overall level of bicoherence decreases (Fig. 2e). In the last cross section ($x = 315$ mm), the bicoherence amplitude has the same level as in the second one (Fig. 2f). In contrast to the second cross section, however, the interaction mainly occurs with low frequencies $f_1 = 1\text{--}20$ kHz and $f_2 = 200\text{--}260$ kHz, which “lifts up” the low-frequency range of the spectrum. A decrease in bicoherence amplitude, which indicates the degree of the quadratic relation in terms of phases, indicates that the region of strongly nonlinear development of the waves begins with cubic, fourth, etc., orders of the nonlinear relation. The transition into the strongly nonlinear region is also indicated by equalization of the power spectrum (see Fig. 1), i.e., spectral energy redistribution occurs due to the nonlinear interaction.

4. Conclusions. The weakly nonlinear region of the laminar–turbulent transition on a sharp cone at hypersonic velocities is considered in the paper by the method of bispectral analysis. The existence of subharmonic resonance at the initial stage of the laminar–turbulent transition at hypersonic velocities is proved for the first time. The interaction occurs in a wide spectral range, and the line of interaction is shifted toward the low-frequency range of the spectrum in the downstream direction as the frequency of the second-mode waves decreases. The nonlinear interaction leading to generation of the harmonic of the second-mode disturbances, described in [8, 10], is also observed.

This work was supported by the Russian Foundation for Fundamental Research (Grant No. 02-01-00141), INTAS (Grant No. 2000-0007), and Air Force Office of Scientific Research (Grant No. F49620-01-0105).

REFERENCES

1. Y. S. Kachanov and V. Y. Levchenko, “The resonance interaction of disturbances at laminar–turbulent transition,” *J. Fluid Mech.*, **138**, 209–247 (1984).
2. W. S. Saric, V. V. Kozlov, and V. Y. Levchenko, “Forced and unforced subharmonic resonance in boundary layer transition,” AIAA Paper No. 84-0007 (1984).
3. A. D. Kosinov, N. V. Semionov, S. G. Shevelkov, and O. I. Zinin, “Experiments on the nonlinear instability of supersonic boundary layers,” in: D. T. Valentine, S. P. Lin, and W. R. C. Phillips (eds.), *Nonlinear Instability of Nonparallel Flows*, Springer-Verlag, New York (1994), pp. 196–205.
4. L. M. Mack, “On the inviscid acoustic-mode instability of supersonic shear flows. Part 1. Two-dimensional waves,” *Theor. Comput. Fluid Dyn.*, **2**, 97–123 (1990).
5. Y. S. Kachanov, V. M. Gilev, and V. V. Kozlov, “Evolution of a spatial wave packet in the boundary layer,” *Izv. Sib. Ord., Akad. Nauk SSSR, Ser. Tekh. Nauk*, Issue 3, No. 13, 12 (1983).
6. A. A. Maslov, A. D. Kosinov, and S. G. Shevelkov, “Experiments on the stability of supersonic laminar boundary layers,” *J. Fluid Mech.*, **219**, 621–633 (1990).
7. A. Popoulis, *Probability, Random Variables, and Stochastic Processes*, McGraw Hill Book, New York (1965).
8. R. L. Kimmel and J. M. Kendall, “Nonlinear disturbances in a hypersonic boundary layer,” AIAA Paper No. 91-0320 (1991).
9. A. I. Semisynov and A. D. Kosinov, “Application of high-order spectra and statistical methods for studying the nonlinear stage of transition in a supersonic boundary layer,” Preprint No. 9-2002, Inst. Theor. Appl. Mech., Sib. Div., Russian Acad. of Sci., Novosibirsk (2002).
10. N. Chokani, “Nonlinear spectral dynamics of hypersonic laminar boundary layer flow,” *Phys. Fluids*, **12**, 3846–3851 (1999).
11. K. F. Stetson, E. R. Thompson, J. C. Donaldson, and L. G. Siler, “Laminar boundary layer stability experiments on a cone at Mach 8. Part 1. Sharp cone,” AIAA Paper No. 83-1761 (1983).
12. D. A. Bountin, A. A. Sidorenko, and A. N. Shipliyuk, “Development of natural disturbances in a hypersonic boundary layer on a sharp cone,” *J. Appl. Mech. Tech. Phys.*, **42**, No. 1, 57–62 (2001).
13. Ch. L. Nikias and M. R. Raghuveer, “Bispectrum estimation: a digital signal processing framework,” *Proc. IEEE*, **75**, No. 7, 5–30 (1987).
14. L. M. Mack, “Stability of axisymmetric boundary layers on sharp cones at hypersonic Mach numbers,” AIAA Paper No. 87-1413 (1987).
15. V. I. Borodulin, Y. S. Kachanov, and D. V. Koptsev, “Experimental study of resonant interactions of instability waves in self-similar boundary layer with an adverse pressure gradient. 3. Broadband disturbances,” *J. Turbulence*, **3**, No. 064, 1–19 (2002).